Revista Mexicana de Astronomía y Astrofísica, **47**, 345–356 (2011)

SPACE REDDENINGS FOR FIFTEEN GALACTIC CEPHEIDS

D. G. Turner,[1] R. F. MacLellan,[2] A. A. Henden,[3] and L. N. Berdnikov[4]

Received 2011 February 24; accepted 2011 June 27

RESUMEN

Derivamos enrojecimientos espaciales para 15 Cefeidas galácticas a partir de datos CCD *BV(RI)*$_C$ desenrojecidos para estrellas tipo AF en las vecindades inmediatas de esas variables, en conjunción con enrojecimientos 2MASS de estrellas tipo BAF en los mismos campos. Analizamos las soluciones potenciales de enrojecimiento utilizando el método de extinción variable para identificar estrellas con distancias y enrojecimientos similares a las de las Cefeidas, muchas de las cuales presentan excesos de color. Hemos modificado ligeramente la relación de color intrínseco *BV(RI)*$_C$ para enanas AF en nuestro análisis, de tal forma que los colores observados para estrellas no enrojecidas en la muestra queden descritos de forma apropiada.

ABSTRACT

Space reddenings are derived for 15 Galactic Cepheids from dereddening CCD *BV(RI)*$_C$ data for AF-type stars in the immediate vicinities of the variables, in conjunction with 2MASS reddenings for BAF-type stars in the same fields. Potential reddening solutions were analyzed using the variable-extinction method to identify stars sharing potentially similar distances and reddenings to the Cepheids, several of which have large color excesses. The intrinsic *BV(RI)*$_C$ color relation for AF dwarfs was modified slightly in the analysis in order to describe better the colors observed for unreddened stars in the samples.

Key Words: methods: observational — stars: variable: Cepheids — ISM: dust, extinction

1. INTRODUCTION

Because of the deleterious effects of interstellar reddening and extinction, it is difficult to establish an empirical picture of the Cepheid instability strip based entirely upon observations of Milky Way Cepheids. The use of extragalactic Cepheids is not necessarily a practical solution to the problem, since the available data for Milky Way Cepheids are generally more extensive and of greater precision, and the effects of internal reddening within other galaxies are not as well established as they are locally. Such considerations justify the continued use of the Galactic sample in studies aimed at establishing reliable intrinsic properties of classical Cepheid variables.

The determination of accurate reddenings for Cepheids has traditionally followed three different routes: (i) from field reddenings of specific objects (e.g., binary, cluster, association, or isolated Cepheids) based upon the analysis of photometric data for early-type stars sharing the same lines of sight, (ii) from observations mainly of bright Cepheids involving photometric parameters designed to be independent of interstellar reddening, and (iii) from using standard reddening laws and a calibrated intrinsic color relation (either observational or model generated) to deredden photometric observations for large samples of Cepheids. Methods (i) and (ii) are the most reliable means of establishing reddenings for individual Cepheids since method (iii) may entail use of period-color relations (e.g., Fernie 1990a,b), which do not account for the intrinsic spread in effective temperature of the Cepheid instability strip and may generate erroneous results (see Turner 1995).

For method (ii), spectroscopic indices related to stellar effective temperature and designed to be independent, or relatively independent, of interstellar and atmospheric extinction include the Γ-index (Kraft 1960; Spencer Jones 1989), which measures

[1]Saint Mary's University, Halifax, Nova Scotia, Canada.
[2]Queen's University, Kingston, Ontario, Canada.
[3]AAVSO, Cambridge, Massachusetts, USA.
[4]Sternberg Astronomical Institute, Moscow, Russia.

the depression of the *G*-band of CH (λ4305) relative to the local continuum, the β-index, which samples the strength of the Hβ Balmer line of hydrogen relative to the surrounding continuum, and the *KHG*-index of Brigham Young University (McNamara & Potter 1969; McNamara, Helm, & Wilcken 1970; Feltz 1972), which measures the strengths of Ca II K (λ3933), Balmer Hδ (λ4101), and the *G*-band through narrow band interference filters in a manner independent of extinction. A more recent technique (Sasselov & Lester 1990) involves the use of line depth ratios between C I and Si II lying on the Brackett continuum near 10728 Å. A similar technique was used by Krockenberger et al. (1998) using spectral lines falling in the red region of Cepheid spectra. Kovtyukh et al. (2008) have taken the technique to its ultimate level of sophistication by using high resolution optical spectra of Cepheids throughout their cycles, in conjunction with stellar atmosphere models, to track their changes in effective temperature, and thus intrinsic broad band color.

The use of close neighbours to deduce reddenings for Cepheids appears to date from its application to the blue companion of δ Cep by Eggen (1951); it has also been used recently for Cepheids studied with the *Hubble Space Telescope* (Benedict et al. 2007). But the existing sample includes only ∼40 Cepheids of known space reddening (Laney & Caldwell 2007). This study presents new space reddenings for 15 Galactic Cepheids derived from CCD $BV(RI)_C$ photometry for stars in the immediate fields of the variables. The goal is to test the feasibility of deriving Cepheid reddenings based upon only $BV(RI)_C$ observations for stars in the fields of the Cepheids, as well as to augment the limited sample of Cepheids with space reddenings. As demonstrated here, the methodology appears to provide useful results that extend the sample of Cepheids with independently derived reddenings.

2. OBSERVATIONAL DATA

The input data for the present study consist of observations of 15 Cepheid fields obtained with the 1.0 m Ritchey-Chrétien telescope of the U.S. Naval Observatory, Flagstaff Station. A Tektronix/SITe, 1024 × 1024 pixel, thinned CCD was used with Johnson system BV and Kron-Cousins system $(RI)_C$ filters to image the fields (e.g., Henden & Munari 2000). Several deep images were obtained for each field, from which average $BV(RI)_C$ magnitudes and colors, with typical uncertainties smaller than $\pm0^m.01$, were extracted for all detectable stars using DAOPHOT (Stetson 1987). Since no *U*-band observations or spectral types are available for the stars in the survey fields, it was necessary to deduce individual reddenings from photometric analyses of two-color diagrams constructed from the $BV(RI)_C$ data. The data are available electronically from A.A.H. via ftp from the American Association of Variable Star Observers website[5].

An often-ignored feature of interstellar reddening is that no single relationship accurately describes it over all regions of the Galaxy (Wampler 1961, 1962; Mathis 1990; Turner 1976a,b, 1989, 1994). Regional variations in the reddening law depend directly upon direction viewed through the Milky Way, vary slowly with Galactic longitude, and are tied to differences in the distribution of particle sizes for dust lying along different lines of sight. The resulting Galactic longitude and latitude dependence of the extinction law affects interstellar reddening studies that implicitly use a relationship of fixed parameterization to describe the extinction in a particular color system, and should be most important for stars of large reddening. Several of the Cepheids in the present sample are heavily reddened, so the extinction laws for the fields of each object were established prior to the analysis by taking advantage of existing studies for regions reasonably close to the program objects (e.g., Johnson 1968; Turner 1976b, 1989, as well as other published studies by the lead author).

Specifically, a reddening slope E_{U-B}/E_{B-V} for the field of each program Cepheid was established from studies by Turner (1976b, 1989) for adjacent regions, and was linked to specific reddening slopes E_{V-I}/E_{B-V} and E_{R-I}/E_{B-V} on the Johnson system using regional reddening curves from Johnson (1968). Those were then converted to reddening slopes E_{V-I}/E_{B-V} and E_{R-I}/E_{B-V} on the Kron-Cousins system using the results of Fernie (1983) and Caldwell et al. (1993). To illustrate the methodology, the results for specific fields studied by Johnson (1968) and exhibiting a range of color excess ratios E_{U-B}/E_{B-V} are shown in Figure 1, where it can be noted that the *I*–band E_{V-I}/E_{B-V} reddening ratios appear to display no significant dependence on visible reddening slope E_{U-B}/E_{B-V}. The Cepheids studied here all lie in fields where the reddening slope does not vary significantly from the locally observed Galactic mean, so specifying the exact reddening ratio for each field proved to be only a minor concern.

3. METHOD OF ANALYSIS

This study presents new space reddenings for 15 Galactic Cepheids derived from two-color dia-

[5] ftp://www.aavso.org/public/calib/.

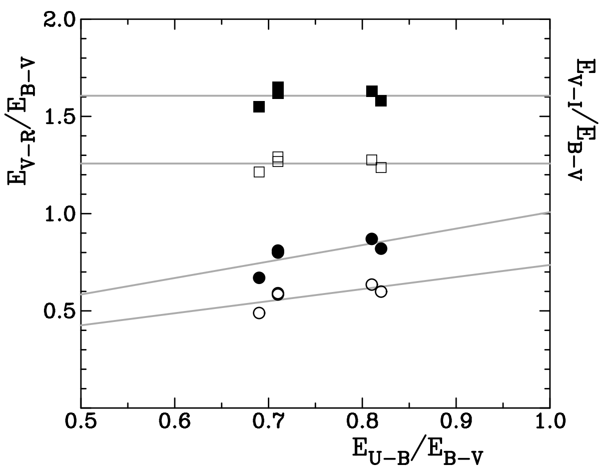

Fig. 1. Derived Johnson system (filled symbols) and Kron-Cousins system (open symbols) reddening ratios E_{V-R}/E_{B-V} (circles, lower) and E_{V-I}/E_{B-V} (squares, upper) for fields studied by Johnson (1968). Gray lines denote the implied dependences on reddening slope E_{U-B}/E_{B-V}.

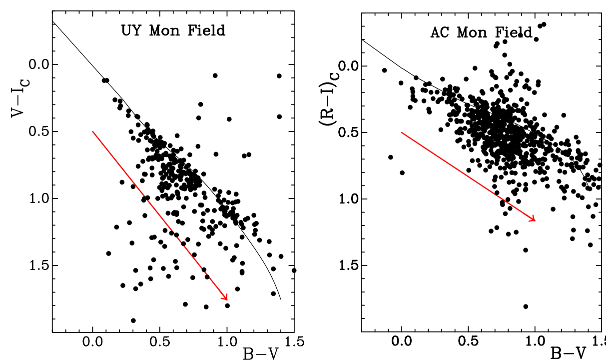

Fig. 2. Two-color diagrams, V–I_C versus B–V for the field of UY Mon (left), and $(R$–$I)_C$ versus B–V for the field of AC Mon (right), showing the intrinsic color relations adopted (solid curves). Reddening lines specific for the fields are shown separately in red for $E_{B-V} = 1.0$, with arrows denoting the direction of increasing reddening. The color figure can be viewed online.

grams, V–I_C versus B–V and $(R$–$I)_C$ versus B–V, constructed from CCD $BV(RI)_C$ photometry for stars in the fields of the variables. Reddening lines appropriate for each field were adopted as indicated above, specifically the adopted reddening slopes E_{U-B}/E_{B-V} were 0.73 for VY Sgr, AY Sgr, and V1882 Sgr, 0.75 for HZ Per and OT Per, 0.76 for FO Cas, IO Cas, EW Aur, YZ CMa, CN CMa, BD Pup, BE Pup, and LR Pup, and 0.77 for UY Mon and AC Mon. The reddening slopes E_{V-I}/E_{B-V} and E_{R-I}/E_{B-V} were next obtained through interpolation and computation with the data of Figure 1, resulting in values on the Kron-Cousins system of $E_{V-I}/E_{B-V} = 1.257$ for all fields and values of E_{R-I}/E_{B-V} of 0.689, 0.677, 0.670, and 0.664, respectively, for the Cepheid fields listed above. Examples are shown in Figure 2, where the derived reddening slopes for UY Mon and AC Mon are $E_{V-I}/E_{B-V} = 1.257$ and $E_{R-I}/E_{B-V} = 0.664$ according to the inferred reddening ratio $E_{U-B}/E_{B-V} = 0.73$. Note that the adopted field reddening lines are unchanging for E_{V-I}/E_{B-V} and exhibit only small variations for E_{R-I}/E_{B-V}.

Initial tests with two-color diagrams using intrinsic $BV(RI)_C$ colors for dwarfs from Caldwell et al. (1993) revealed small anomalies in the inferred E_{B-V} reddenings derived from the two diagrams, as well as an overabundance of unreddened and negatively-reddened stars relative to the intrinsic relation, not explainable as luminosity effects (Caldwell et al. 1993). Such non-physical results suggested the need for slight corrections to the intrinsic colors used with the present data sets, which are normalized to the Kron-Cousins system. Small adjustments to the intrinsic relations for late B-type and A-type dwarfs to make them bluer were therefore tried, using alternative intrinsic colors from Johnson (1966) adjusted to the Cape system (Fernie 1983). That produced greater consistency in the derived reddenings and better agreement for unreddened stars, and was adopted throughout the remainder of the study. The intrinsic colors corresponding to such changes are presented in Table 1 for reference purposes, where they are compared with the Caldwell et al. (1993, SAAO) colors for dwarfs, which were adopted for all other stars. Given that the analysis was restricted to stars that dereddened uniquely to the AF-dwarf relation, the modification affects the resulting space reddenings, but only to a minor extent. Likely B-type stars in the field of each Cepheid were only used when analyzing 2MASS colors for the stars.

Reddening lines run nearly parallel to the intrinsic relations for B-dwarfs and KM-dwarfs, particularly in V–I_C versus B–V diagrams, which is why the analysis was restricted to stars indicated to be likely AF-dwarfs, which are reasonably plentiful in each field. The slope of the intrinsic relation for AF-dwarfs relative to the effects of interstellar reddening in the $BV(RI)_C$ system results in sufficient separation, particularly in $(R$–$I)_C$ relative to B–V, to produce unique photometric dereddening solutions for

TABLE 1

INTRINSIC $BV(RI)_C$ COLORS FOR DWARFS

$(B–V)_0$	$(V–I)_0$	$(V–I)_0$ SAAO	$(R–I)_0$	$(R–I)_0$ SAAO
−0.24	−0.259	−0.237	−0.157	−0.158
−0.23	−0.248	−0.221	−0.150	−0.146
−0.22	−0.236	−0.206	−0.143	−0.134
−0.21	−0.225	−0.193	−0.136	−0.123
−0.20	−0.214	−0.181	−0.129	−0.114
−0.19	−0.203	−0.170	−0.121	−0.105
−0.18	−0.192	−0.159	−0.114	−0.097
−0.17	−0.180	−0.149	−0.107	−0.089
−0.16	−0.169	−0.140	−0.100	−0.082
−0.15	−0.158	−0.131	−0.092	−0.076
−0.14	−0.147	−0.122	−0.085	−0.070
−0.13	−0.136	−0.114	−0.078	−0.064
−0.12	−0.124	−0.106	−0.071	−0.059
−0.11	−0.113	−0.098	−0.064	−0.053
−0.10	−0.102	−0.090	−0.056	−0.048
−0.09	−0.091	−0.082	−0.049	−0.043
−0.08	−0.080	−0.074	−0.042	−0.039
−0.07	−0.068	−0.066	−0.035	−0.034
−0.06	−0.057	−0.057	−0.028	−0.029
−0.05	−0.046	−0.049	−0.020	−0.024
−0.04	−0.035	−0.040	−0.013	−0.020
−0.03	−0.024	−0.031	−0.006	−0.015
−0.02	−0.012	−0.022	+0.001	−0.010
−0.01	−0.001	−0.013	+0.008	−0.005
+0.00	+0.010	−0.004	+0.015	+0.000
+0.01	+0.021	+0.006	+0.021	+0.005
+0.02	+0.032	+0.016	+0.027	+0.010
+0.03	+0.043	+0.026	+0.033	+0.016
+0.04	+0.055	+0.037	+0.040	+0.021
+0.05	+0.066	+0.048	+0.046	+0.026
+0.06	+0.077	+0.059	+0.053	+0.032
+0.07	+0.088	+0.070	+0.059	+0.038
+0.08	+0.100	+0.081	+0.066	+0.043
+0.09	+0.111	+0.093	+0.072	+0.049
+0.10	+0.122	+0.105	+0.078	+0.055
+0.11	+0.133	+0.117	+0.084	+0.061
+0.12	+0.144	+0.129	+0.090	+0.068
+0.13	+0.156	+0.141	+0.095	+0.074
+0.14	+0.167	+0.153	+0.101	+0.080
+0.15	+0.178	+0.166	+0.106	+0.086
+0.16	+0.189	+0.179	+0.112	+0.093
+0.17	+0.200	+0.191	+0.117	+0.099
+0.18	+0.212	+0.204	+0.122	+0.106
+0.19	+0.223	+0.217	+0.127	+0.112
+0.20	+0.234	+0.230	+0.133	+0.119
+0.21	···	+0.243	+0.138	+0.125
+0.22	···	+0.256	+0.143	+0.132
+0.23	···	+0.269	+0.148	+0.138
+0.24	···	+0.281	+0.154	+0.144
+0.25	···	+0.294	+0.159	+0.151
+0.26	···	+0.307	+0.164	+0.157
+0.27	···	+0.320	+0.170	+0.164
+0.28	···	+0.332	+0.175	+0.170
+0.29	···	+0.345	+0.180	+0.176
+0.30	···	+0.357	+0.185	+0.182

each star, and the use of two separate color-color diagrams provides independent estimates for the intrinsic color of each star, although greater precision is obtained with solutions from the $(R–I)_C$ versus $B–V$ diagram alone, because the angle between the intrinsic relation and typical reddening lines is larger. Infrared JHK_s observations exist for most stars (Cutri et al. 2003) from the Two Micron All Sky Survey (2MASS, Skrutskie et al. 2006), and confirm the adopted reddenings from $BV(RI)_C$ data, although the scatter in 2MASS JHK_s colors tends to be rather significant, larger than in UBV color-color diagrams (Turner 1976a).

Typical companions and progenitors of Cepheids are B-type stars (Turner 1984), which are rare enough that their occurrence in the field of a Cepheid raises the possibility of a physical association. AF-type stars, on the other hand, are a more common constituent of Galactic star fields (McCuskey 1965), so the possibility of their physical association with a nearby Cepheid is reduced, but not necessarily to zero. In many of our program fields some of the stars identified as likely AF-type may be associated with the Cepheid of interest, but that was not explored here since there are no catalogued star clusters in the fields, although the regions around UY Mon, BE Pup, YZ CMa, and VY Sgr appear to contain faint anonymous clusters, and BD Pup and FO Cas are located in bright groups of surrounding stars.

The additional scatter in Figure 2 illustrates some of the problems associated with dereddening stars in $BV(RI)_C$ color-color diagrams. Such scatter for a small proportion of stars is a common characteristic of color-color diagrams, including those in UBV and those used for 2MASS photometry, and is readily explained in most cases by observational error, typically one or more of the magnitudes in the observed colors falling too close to the survey limits. At bright magnitude limits the typical stars encountered in Galactic star fields are A dwarfs and

GK giants (McCuskey 1965), but the demographic changes as the magnitude limits increase, and faint, nearby degenerate stars and M dwarfs begin to compound the picture with their unusual colors and larger measuring uncertainties. Emission, binarity, overly bright stars suffering from image saturation, objects lying away from the main sequence (Caldwell et al. 1993), and low quality observations for faint stars all combine to generate scatter in such plots, but using two separate color-color diagrams and limiting the analysis to stars fainter than the bright survey limits and brighter than the faint survey limits assures that likely AF dwarfs are identified properly. They are the small fraction of objects that deredden uniquely to the intrinsic relation for such stars in Figure 2, as confirmed by their JHK_s colors.

The derived reddenings for stars analyzed in each field were adjusted to equivalent color excesses for a B0 star according to their inferred intrinsic colors and the dependence of reddening on intrinsic color summarized by Fernie (1963). Interstellar extinction affects the effective wavelengths of broad band BV filters differently according to the continuum of the star being observed, such that a typical Cepheid of, say, $(B-V)_0 = 0.60$ reddened by $E(B-V) = 0.90$ suffers identical extinction to a B0 dwarf star of $(B-V)_0 = -0.30$ reddened by $E(B-V) = 0.97$ (cf. η factor of Fernie 1963). Such adjustments are necessary when comparing reddenings of stars across a wide range of intrinsic color. Zero-age main sequence (ZAMS) values of M_V as a function of intrinsic $(B-V)_0$ color (Turner 1976a, 1979) were also assigned to each star from the photometric dereddening solutions in order to provide estimates, or at least underestimates, of apparent distance modulus, V–M_V, for the stars in each field. The stars were then plotted in a variable-extinction diagram, such as those for each field summarized in Figure 3, as a means of assessing the likely space reddening of each Cepheid. Figure 3 represents only a portion of each variable-extinction diagram, namely the most heavily-populated regions associated with the expected parameters for each Cepheid.

Mean $\langle B\rangle$ and $\langle V\rangle$ magnitudes are available for each Cepheid from Berdnikov (2007) and the present study, and rough estimates of reddening and luminosity were made from older, published period-color (e.g., Fernie 1990a,b) and period-luminosity (e.g., Turner 1992) relations, which do not differ substantially from more recent results (Turner 2001, 2010). It was then possible to establish roughly where in each variable-extinction diagram the parameters for the Cepheid should fall, keeping in mind that an extremely liberal interpretation of such "predictions" is essential to avoid biasing the results. Some of the sample Cepheids are suspected Type II objects or overtone pulsators, for example, which affects estimates of both reddening and luminosity. Generous uncertainties of ± 0.1 or more in E_{B-V} and ± 1 in M_V were therefore assumed in the analysis. Note that the "predictions" for IO Cas, FO Cas, and V1882 Sgr are inconsistent with expectations for classical Cepheids (they have larger predicted distance moduli than those for surrounding stars of similar reddening), which means that they are potential Type II objects. The situation for HZ Per, BD Pup, and OT Per is more ambiguous.

All such information is needed in order to establish which stars in the field of each Cepheid are useful for deriving its space reddening. In the case of UY Mon, for example, the estimated distance and reddening for the Cepheid associate it with the group of slightly reddened stars at $E_{B-V} \simeq 0.1$, $(V$–$M_V)_0 \simeq$ 11–12 ($d \simeq$ 1.6–2.5 kpc), but less distant and less reddened than stars of $E_{B-V} \simeq 0.5$, $(V$–$M_V)_0 \simeq$ 12.5–13 ($d \simeq$ 3–4 kpc), in its vicinity. The best match is therefore to the 4 stars within $5'$ of UY Mon that are reddened by $E_{B-V} \simeq 0.1$. Other cases are more complex because of the patchy reddening that permeates most fields, but have been resolved by considering only stars close to each Cepheid.

What appears to be a continuous run of reddening with distance in some fields results from the patchy extinction in each field combined with larger-than-average uncertainties in the inferred color excesses, E_{B-V}. The extinction associated with most Galactic star fields is typically associated with individual dust clouds dispersed along the line of sight (Turner 1994). But large uncertainties in reddening can confuse the picture. Figure 4 presents the results of a simulation of such circumstances in a field where the scatter in the color excesses is taken to be ± 0.05, with associated uncertainties in absolute magnitude of ± 0.5, both quantities being applied randomly to the test points. Star densities were assumed constant as a function of distance, and the input parameters included specific amounts of reddening and extinction arising in discrete dust clouds located along the line of sight at distances of 0.5 pc, 0.9 pc, and 1.1 pc, producing mean color excesses of $E_{B-V} = 0.2$, 0.5, and 0.7, respectively. An extinction law with $R = 3.0$ is depicted for the last group. The parameters, in particular the adopted scatter, were chosen in order to produce the greatest complexity in the resulting variable-extinction diagram. The resulting scatter produces results similar

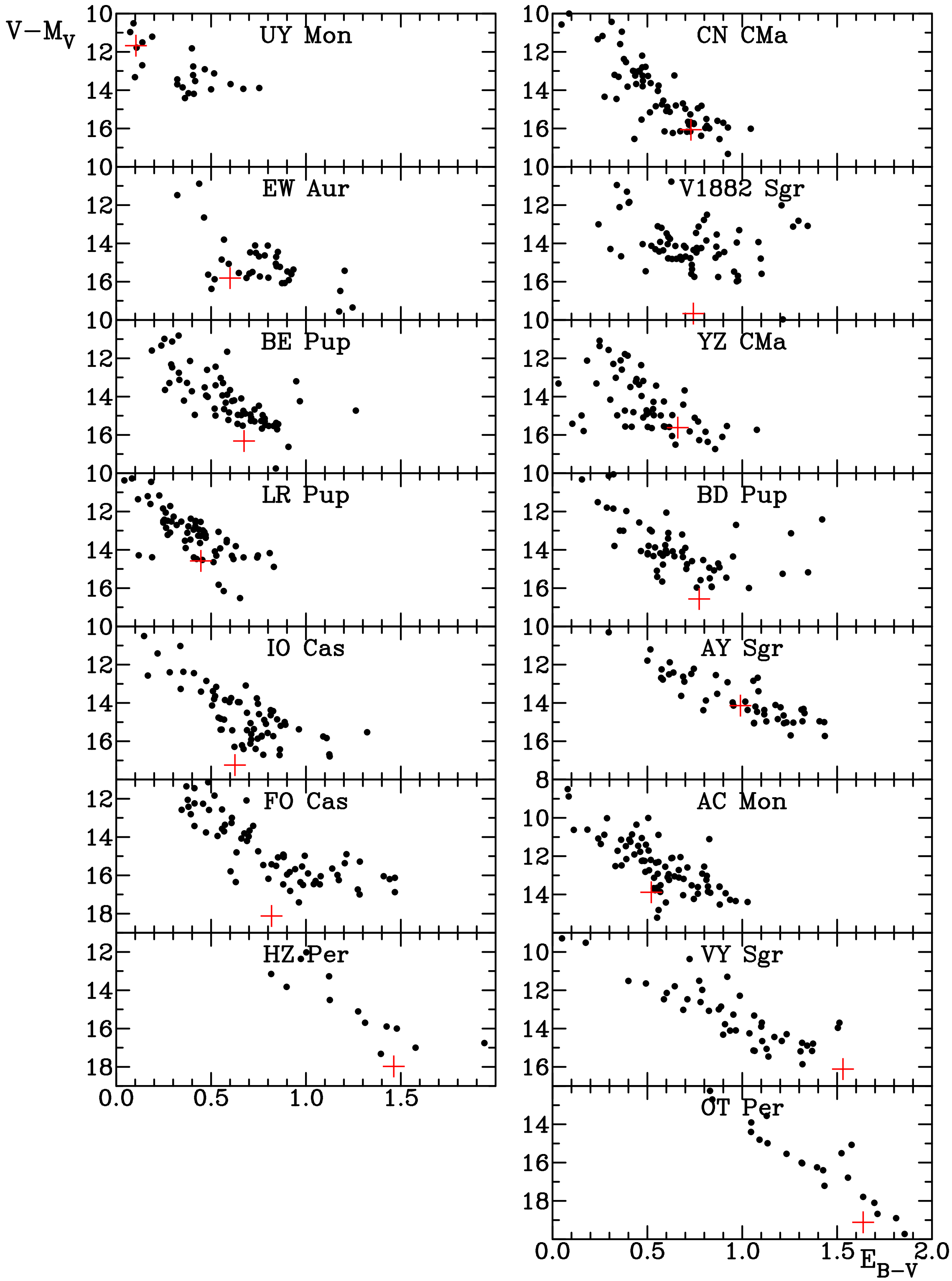

Fig. 3. Variable-extinction diagrams for the fields examined in this study, identified by the Cepheid of interest. Filled symbols denote AF stars near each Cepheid, and red plus signs are "predictions" for the Cepheid parameters. The color figure can be viewed online.

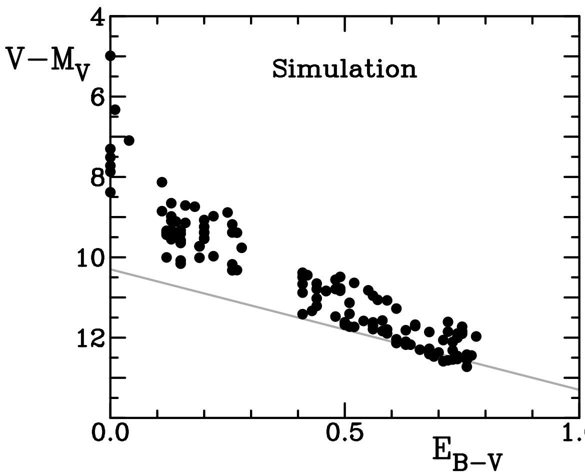

Fig. 4. A simulated variable-extinction diagram for a star field where the reddening increases with distance according to dust clouds producing $E_{B-V} = 0.20$, 0.50, and 0.70 located at distances of 0.5 kpc, 0.9 kpc, and 1.1 kpc, respectively, with associated uncertainties in E_{B-V} of ±0.05 and in M_V of ±0.5. The gray line denotes a standard reddening law of $R = A_V/E_{B-V} = 3.0$ for stars at a distance of 1.1 kpc.

to some of the variable-extinction diagrams of Figure 3.

The large range of inferred reddenings for field stars near each Cepheid was reduced further through an analysis of 2MASS observations (Cutri et al. 2003) for likely BAF-type stars in the same fields, analyzed in similar fashion to that employed by Turner et al. (2008) and Turner (2011). 2MASS observations were used separately without combination with the $BV(RI)_C$ photometry in order to avoid potential zero-point problems. The observed J–H and H–K_s colors for stars lying within 5′ of each Cepheid are shown in Figure 5, and were compared with the intrinsic relation for main-sequence stars in the 2MASS system (Turner 2011), adjusted with a reddening slope $E_{H-K}/E_{J-H} = 0.49$ from Turner (2011). Multiple solutions in some cases, e.g., UY Mon and HZ Per, were resolved with reference to the variable-extinction diagrams and "predicted" values, and best fits were made by trial and error by establishing reddenings for which likely BAF-type stars had colors distributed randomly about the reddened intrinsic relation.

The JHK_s colors generate independent E_{B-V} reddenings for the stars in the Cepheid fields, with the advantage of being more closely tied to B-type stars in the fields, stars that lie blueward of the "kink" in the intrinsic relation and that may share a common origin with the Cepheid. The reddenings have slightly larger uncertainties because of larger photometric scatter in the observations (by factors of 3–5 relative to the $BV(RI)_C$ photometry) in combination with the correction from infrared to optical reddening. They are nevertheless crucial for narrowing the range of potential color excesses for some of the sample Cepheids, such as IO Cas. A few objects in the sample appear to be Type II Cepheids, but that does not affect the results. In most cases the implied reddening near the Cepheid is fairly evident.

4. RESULTS

The results of the variable-extinction studies of the sample Cepheids are presented in Table 2, which lists the inferred space reddening for each Cepheid derived from likely AF-type stars lying within different angular radii, from 2′ to 5′ distant, and the reddening inferred from 2MASS JHK_s colors for stars within 5′ of the Cepheid. The adopted color excess in each case, Column 8, was the average for all AF-type stars lying within 5′ of the Cepheid and of comparable inferred distance, and the resulting reddening, which is equivalent to that for a star of spectral type B0, was converted in the last column of the table to a value appropriate for the derived intrinsic color of the Cepheid, again using the relationship of Fernie (1963). The number of stars used to obtain the space reddening is listed in the second last column of Table 2. In rich fields that number is of order ∼10–20, whereas in more poorly populated regions or fields with a larger spread in reddening, less than half a dozen reference stars were available. Two solutions are presented for UY Mon, for reasons indicated later, although the adopted solution for the Cepheid is the first.

It is worth noting that the 2MASS reddenings fall closer to the converted color excess for the Cepheid than to the B0-star reddenings. A reasonable explanation lies in the fact that the BAF-star reddenings in a 2MASS color-color diagram tend to be dominated by the AF stars, particularly likely F-type stars, since B-type stars are less common in the small fields analyzed and are potentially affected by circumstellar effects (Turner 2011). The 2MASS reddenings are also important for providing confirmation of the relationship used to convert B0-star color excesses to those appropriate for a star with the average unreddened colors of the Cepheid, which are very similar to F-type dwarfs in the 2MASS samples.

The derived intrinsic colors are presented in Table 3, which also provides in Column 3 the variable

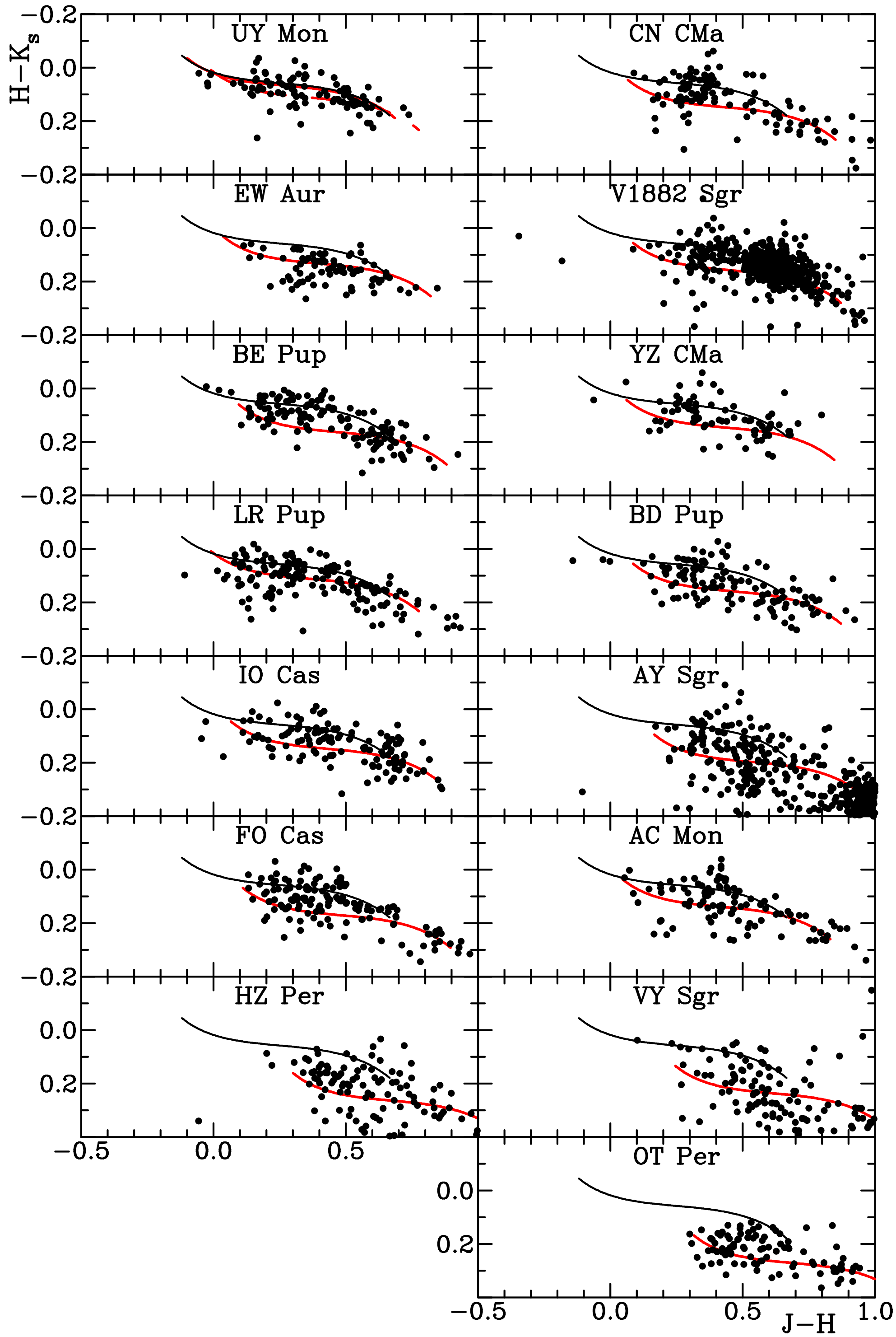

Fig. 5. 2MASS color-color diagrams, H–K_s versus J–H, for stars within 5′ of each Cepheid, from observations by Cutri et al. (2003). The intrinsic relation for main sequence stars is plotted as a black line, while red lines depict the adopted reddening for stars associated with the Cepheids, from Column 7 of Table 2. The dashed red line for UY Mon represents the alternate solution for that field. The color figure can be viewed online.

TABLE 2

SPACE REDDENINGS FOR CEPHEID FIELDS

Cepheid	log P	E_{B-V}(B0) $< 2'$	E_{B-V}(B0) $< 3'$	E_{B-V}(B0) $< 4'$	E_{B-V}(B0) $< 5'$	E_{B-V} 2MASS	E_{B-V}(B0) Adopted	No. Stars	E_{B-V}(Cδ)
UY Mon	0.380	···	0.09	0.09	0.12 ± 0.01	0.07 ± 0.07	0.12 ± 0.01	4	0.11 ± 0.01
UY Mon[1]	···	···	0.42	0.44 ± 0.03	0.43 ± 0.02	0.37 ± 0.07	0.43 ± 0.02	3	···
CN CMa	0.390	0.62 ± 0.02	0.65 ± 0.02	0.66 ± 0.02	0.67 ± 0.02	0.63 ± 0.12	0.67 ± 0.02	11	0.63 ± 0.02
EW Aur	0.425	0.52	0.63 ± 0.06	0.61 ± 0.04	0.61 ± 0.04	0.53 ± 0.08	0.61 ± 0.04	6	0.58 ± 0.03
V1882 Sgr	0.433	0.60 ± 0.01	0.68 ± 0.03	0.70 ± 0.02	0.68 ± 0.02	0.69 ± 0.05	0.68 ± 0.02	20	0.64 ± 0.01
BE Pup	0.458	0.80	0.72 ± 0.04	0.69 ± 0.03	0.68 ± 0.02	0.73 ± 0.12	0.68 ± 0.02	20	0.64 ± 0.02
YZ CMa	0.499	···	0.71 ± 0.10	0.64 ± 0.09	0.60 ± 0.03	0.61 ± 0.07	0.60 ± 0.03	10	0.56 ± 0.03
LR Pup	0.523	0.44	0.47 ± 0.02	0.46 ± 0.01	0.45 ± 0.01	0.37 ± 0.07	0.45 ± 0.01	14	0.42 ± 0.01
BD Pup	0.593	0.63 ± 0.03	0.71 ± 0.03	0.74 ± 0.03	0.72 ± 0.02	0.69 ± 0.08	0.72 ± 0.02	19	0.67 ± 0.02
IO Cas	0.748	0.74	0.64 ± 0.03	0.62 ± 0.03	0.63 ± 0.03	0.63 ± 0.08	0.63 ± 0.03	14	0.59 ± 0.02
AY Sgr	0.818	···	1.04 ± 0.02	1.02 ± 0.04	1.00 ± 0.03	0.97 ± 0.05	1.00 ± 0.03	8	0.94 ± 0.02
FO Cas	0.832	0.99	0.99	0.83 ± 0.07	0.82 ± 0.06	0.78 ± 0.14	0.82 ± 0.06	7	0.76 ± 0.05
AC Mon	0.904	···	0.61	0.61 ± 0.02	0.59 ± 0.02	0.56 ± 0.05	0.59 ± 0.02	5	0.55 ± 0.01
HZ Per	1.052	1.39	1.39	1.48 ± 0.07	1.48 ± 0.05	1.42 ± 0.10	1.48 ± 0.05	4	1.36 ± 0.04
VY Sgr	1.132	···	1.50	1.41 ± 0.04	1.35 ± 0.04	1.24 ± 0.15	1.35 ± 0.04	3	1.24 ± 0.04
OT Per	1.416	···	1.70	1.52 ± 0.11	1.52 ± 0.09	1.47 ± 0.12	1.52 ± 0.09	5	1.39 ± 0.08

[1]Alternate solution for stars of large reddening near UY Mon.

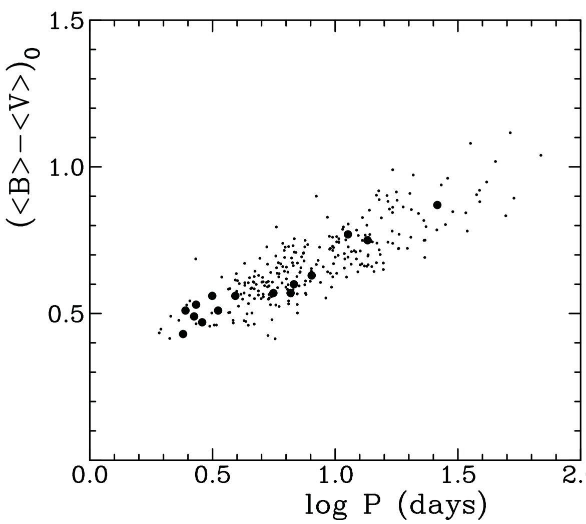

Fig. 6. Derived intrinsic $\langle B\rangle$–$\langle V\rangle$ colors for sample Cepheids (large symbols) relative to other Cepheids with derived reddenings (small symbols, Turner 2001), as a function of pulsation period.

star type designation for the object from the *General Catalogue of Variable Stars* (Samus et al. 2004). Type II Cepheids are designated as CWB for short period (1–8 days) BL Herculis variables, and CWA for longer period (8–20 days) W Virginis stars. The intrinsic $(\langle B\rangle$–$\langle V\rangle)_0$ colors are plotted in Figure 6 relative to a set of similar intrinsic colors calibrated relative to other Cepheids with field reddenings (binary, cluster or association members) and Cepheids with reddenings derived using reddening-free indices (Turner 2001).

All of the program stars studied here appear to have intrinsic colors consistent with those of classical Galactic Cepheids, despite remaining questions about the true population status for some of them. The spread in color at a given value of pulsation period P for the reference sample can be attributed to the natural width of the Cepheid instability strip, and in a few cases to erroneous reddenings. The location of individual Cepheids in our sample relative to the hot (blue) and cool (red) edges of the strip, if used in conjunction with light amplitude and rate of period change, provides useful information about what stage the Cepheids have reached in their evolution (Turner et al. 2006).

Figure 7 plots the inferred $(R$–$I)_J$ colors for our sample Cepheids relative to their $(\langle B\rangle$–$\langle V\rangle)_0$ colors, transposed from $(R$–$I)_C$ using the relationships of Fernie (1983). Included are inferred colors for AFGK supergiants from Johnson (1966), in similar fashion to the analysis of Dean et al. (1978). There is good agreement of the derived intrinsic colors for sample Cepheids with the colors expected for supergiant stars, with the exception of V1882 Sgr and YZ CMa. Both objects have faint optical companions that may contaminate the $(RI)_C$ photometry, so the results of Figure 7 do not necessarily indicate a significant difference in color between classical and Type II Cepheids. The data also indicate the general success of the procedure adopted in this study. The temperature spread of the instability strip is less marked in intrinsic $(R$–$I)_J$ and $(R$–$I)_C$ colors than in $(\langle B\rangle$–$\langle V\rangle)_0$ color, as expected.

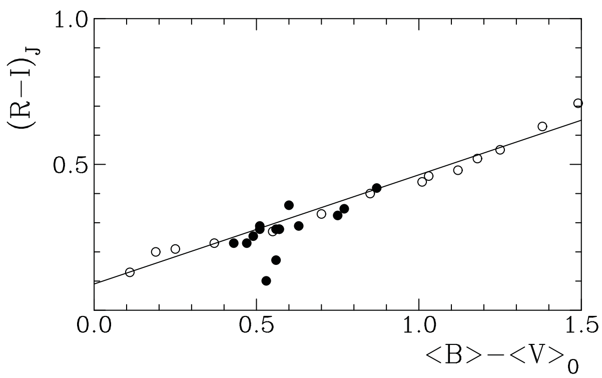

Fig. 7. Derived Johnson system $(R–I)_J$ colors for sample Cepheids (filled circles) relative to intrinsic $(\langle B\rangle–\langle V\rangle)_0$ colors, with derived colors for AFGK supergiants from Johnson (1966) plotted for reference purposes as open circles. The line is a fitted relation for the supergiants. The anomalous Cepheids are V1882 Sgr and YZ CMa.

TABLE 3

UNREDDENED $BV(RI)_C$ COLORS FOR SAMPLE CEPHEIDS

Cepheid	log P	Type	$\langle B\rangle–\langle V\rangle$	$V–R_C$	$V–I_C$	Deduced Type
UY Mon	0.380	DCEPS	+0.43	+0.28	+0.51	DCEPS[1]
CN CMa	0.390	CWB:	+0.51	+0.33	+0.61	DCEP
EW Aur	0.425	DCEP	+0.49	+0.29	+0.54	DCEP
V1882 Sgr	0.433	CEP	+0.53	+0.30	+0.42	CWB
BE Pup	0.458	CWB:	+0.47	+0.29	+0.52	DCEP
YZ CMa	0.499	CWB:	+0.56	+0.28	+0.46	CWB?
LR Pup	0.523	CEP	+0.51	+0.32	+0.59	DCEP
BD Pup	0.593	DCEP	+0.56	+0.36	+0.63	DCEP
IO Cas	0.748	DCEP	+0.57	+0.36	+0.63	CWB?
AY Sgr	0.818	DCEP	+0.57	+0.31	+0.58	DCEP
FO Cas	0.832	DCEP	+0.60	+0.44	+0.78	CWB?
AC Mon	0.904	DCEP	+0.63	+0.35	+0.63	DCEP
HZ Per	1.052	DCEP	+0.77	+0.40	+0.73	DCEP
VY Sgr	1.132	DCEP	+0.75	+0.43	+0.74	DCEP
OT Per	1.416	DCEP	+0.87	+0.49	+0.88	DCEP

[1]Fundamental mode pulsation likely.

With regard to the variable star designations for specific objects in Table 3, the short period Cepheids UY Mon and CN CMa are solar-metallicity stars according to Diethelm (1990), who derived reddenings of $E_{B-V} = 0.15 \pm 0.08$ and 0.61 ± 0.10, respectively, for the stars from Walraven photometry. Both values are consistent with the present results, although of lower precision. UY Mon is an s-Cepheid, its light curve being indistinguishable from a sine wave, many of which are overtone pulsators, yet fundamental mode pulsation provides the simplest solution to the variable-extinction study presented here (Figure 3), provided it is a classical Cepheid. CN CMa is a suspected Type II Cepheid because of its unusually large amplitude for a short-period pulsator, but that designation is not consistent with its photometric solar metallicity (Diethelm 1990) or the variable-extinction analysis. Type II Cepheids are known to display a wide range of abundances, from solar to below solar (Harris 1981), so that is not necessarily a good criterion to decide Population type for CN CMa. A better case for it being a classical Cepheid lies in the variable-extinction results (Figure 3). Its $(RI)_C$ and $(RI)_J$ colors are also consistent with those of a classical Cepheid (Figure 7), which is the designation preferred here.

For four of the sample objects the field star variable-extinction data produce results indicating that the Cepheid's luminosity may have been overestimated in the analysis, i.e., it might be a Type II object. The Cepheids are V1882 Sgr, BE Pup, IO Cas, and FO Cas. The latter two objects are identified as classical Cepheids in the GCVS, so either the variable-extinction results for them are anomalous or the classification of the stars is erroneous. The latter possibility is suspected here, so their deduced types as Type II Cepheids in the last column of Table 3 reflect the results of the variable-extinction analysis. V1882 Sgr has the characteristic light curve of a Cepheid, but is of uncertain type. The variable-extinction results suggest that it is a Type II object, while its $V(RI)_C$ colors (Table 3) are slightly bluer than those of classical Cepheids in the sample, which may indicate a metal-poor object. The "CEP" designation for the star in the GCVS is presumably preliminary, and it appears likely to be a Type II object. Similarly, the variable-extinction results for BE Pup are consistent with either a classical or Type II Cepheid, while its $V(RI)_C$ colors (Table 3) are similar to those of classical Cepheids in the sample. BE Pup is also a double-mode pulsator (Wils & Otero 2004), which is suggestive of a classical Cepheid, our preferred designation.

YZ CMa is suspected to be a classical Cepheid according to the variable-extinction analysis, but its $V(RI)_C$ colors are also slightly bluer than those of other classical Cepheids. The "CWB": designation in the GCVS may therefore be correct, although further study is needed to resolve the question. In general, the studies summarized here consistently tend to identify most sample objects (11/15) as classical Cepheids. Two of the likely Type II objects, V1882 Sgr and YZ CMa, appear slightly bluer in $V–R_C$ and $V–I_C$ than other Cepheids in the sample, but the photometry for both stars may suffer from contamination by close companions, so their distinctive dif-

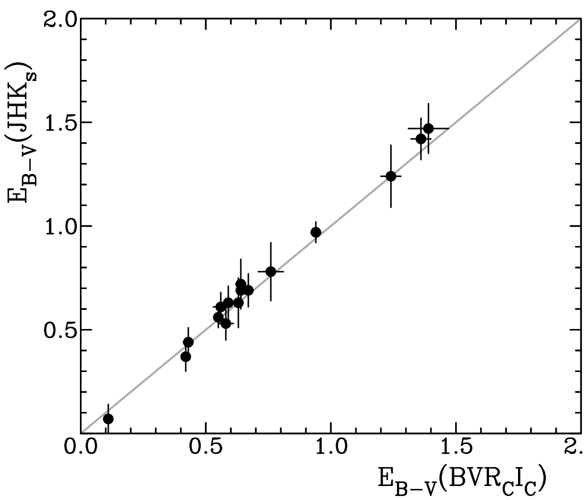

Fig. 8. Comparison of derived 2MASS reddenings, with their uncertainties, for the Cepheids in our sample with the color-corrected broad band $BV(RI)_C$ reddenings. The gray line represents expectations for an exact match.

ference in color cannot be considered definitive. Detailed atmospheric abundance studies of both stars should help to solidify their classifications and establish if there are obvious differences in color between classical and Type II Cepheids.

Figure 8 plots the inferred 2MASS reddenings for our sample Cepheids relative to their broad band $BV(RI)_C$ reddenings, where we have included the second result for the UY Mon field because of the obvious separation in Figures 3 and 5 of stars of small reddening from those of large reddening, for which separate solutions were obtained. The close agreement of both sets of reddenings in Figure 8 indicates that the two techniques are of comparable reliability for establishing field reddenings of Galactic objects, although there is clearly greater precision in the $BV(RI)_C$ color excesses.

5. DISCUSSION

The present study was undertaken as a feasibility test of the use of CCD $BV(RI)_C$ photometry for studying the space reddening of Galactic Cepheids. The $BV(RI)_C$ data by themselves were sometimes insufficient to define the field reddenings of each Cepheid unambiguously, but the addition of 2MASS reddenings and initial "predictions" guided the process successfully. The number of Galactic Cepheids of well-established field reddening has been increased from 40 (Laney & Caldwell 2007) to 55 by this study, and the sample now includes a few Type II Cepheids, some of which appear to display slightly bluer intrinsic $(V–R)_C$ and $(V–I)_C$ colors relative to their classical Cepheid cousins. A comparable test using reddenings derived from 2MASS JHK_s colors indicates that the 2MASS survey may also be suitable for the derivation of space reddenings, for a variety of stellar types and not just Cepheids. Further studies of that possibility have already been initiated (Majaess et al. 2008a,b).

The results of this study have already been used in a preliminary mapping of the Cepheid instability strip using Cepheid reddenings tied to space reddenings and spectroscopic reddenings of Galactic Cepheids (Turner 2001), the results of which can be seen in the data plotted in Figure 6. The addition of *U*-band observations would have assisted the analysis considerably, but it is important to note that accurate Johnson system *U*-band observations are difficult to obtain with some CCD/filter combinations (see comments by Turner 2011). Despite that, the success of the present study using both $BV(RI)_C$ and JHK_s photometry should spur further investigations that take advantage of existing survey photometry to study the reddening in interesting Galactic star fields.

The present study was supported in part by research funding awarded through the Natural Sciences and Engineering Research Council of Canada (NSERC), through the Russian Foundation for Basic Research (RFBR), and through the program of Support for Leading Scientific Schools of Russia. This publication makes use of data products from the Two Micron All Sky Survey, which is a joint project of the University of Massachusetts and the Infrared Processing and Analysis Center/California Institute of Technology, funded by the National Aeronautics and Space Administration and the National Science Foundation.

REFERENCES

Benedict, G. F., et al. 2007, AJ, 133, 1810
Berdnikov, L. N. 2007, http://www.sai.msu.su/groups/cluster/CEP/PHE/
Caldwell, J. A. R., Cousins, A. W. J., Ahlers, C. C., van Wamelen, P., & Maritz, E. J. 1993, South African Astron. Obs. Circ., 15, 1
Cutri, R. M., et al. 2003, The IRSA 2MASS All-Sky Point Source Catalog of Point Sources, NASA/IPAC Infrared Science Archive
Dean, J. F., Warren, P. R., & Cousins, A. W. J. 1978, MNRAS, 183, 569
Diethelm, R. 1990, A&A, 239, 186
Eggen, O. J. 1951, ApJ, 113, 367
Feltz, K. A., Jr. 1972, PASP, 84, 497

Fernie, J. D. 1963, AJ, 68, 780
_________. 1983, PASP, 95, 782
_________. 1990a, ApJS, 70, 153
_________. 1990b, ApJ, 354, 295
Harris, H. C. 1981, AJ, 86, 719
Henden, A. A., & Munari, U. 2000, A&AS, 143, 343
Johnson, H. L. 1966, ARA&A, 4, 193
_________. 1968, in Nebulae and Interstellar Matter, ed. B. L. Middlehurst & L. H. Aller (Chicago: Univ. Chicago Press), 167
Kovtyukh, V. V., Soubiran, C., Luck, R. E., Turner, D. G., Belik, S. I., Andrievsky, S. M., & Chekhonadskikh, F. A. 2008, MNRAS, 389, 1336
Kraft, R. P. 1960, ApJ, 131, 330
Krockenberger, M., et al. 1998, in ASP Conf. Ser. 154, Cool Stars, Stellar Systems, and the Sun, ed. R. A. Donahue & J. A. Bookbinder (San Francisco: ASP), 791
Laney, C. D., & Caldwell, J. A. R. 2007, MNRAS, 377, 147
Majaess D. J., Turner D. G., & Lane D. J. 2008a, MNRAS, 390, 1539
Majaess D. J., Turner D. G., Lane D. J., & Moncrieff, K. A. 2008b, J. Am. Ass. Variable Star Obs., 36, 90
Mathis, J. S. 1990, ARA&A, 28, 37
McCuskey, S. W. 1965, in Galactic Structure, ed. A. Blaauw & M. Schmidt (Chicago: Univ. Chicago Press), 1
McNamara, D. H., Helm, T. M., & Wilcken, S. K. 1970, PASP, 82, 293
McNamara, D. H., & Potter, D. 1969, PASP, 81, 545
Samus, N. N., et al. 2004, Combined Catalog of Variable Stars (Moscow: Inst. of Astronomy of Russian Academy of Sciences)
Sasselov, D. D., & Lester, J. B. 1990, ApJ, 360, 227
Skrutskie, M. F., et al. 2006, AJ, 131, 1163
Spencer Jones, J. H. 1989, MNRAS, 238, 269
Stetson, P. B. 1987, PASP, 99, 191
Turner, D. G. 1976a, AJ, 81, 97
_________. 1976b, AJ, 81, 1125
_________. 1979, PASP, 91, 642
_________. 1984, JRASC, 78, 229
_________. 1989, AJ, 98, 2300
_________. 1992, AJ, 104, 1865
_________. 1994, RevMexAA, 29, 163
_________. 1995, in ASP Conf. Ser. 83, Astrophysical Applications of Stellar Pulsation, ed. Stobie, R. S. & Whitelock, P.-A. (San Francisco: ASP), 256
_________. 2001, Odessa Astron. Publ., 14, 166
_________. 2010, Ap&SS, 326, 219
_________. 2011, RevMexAA, 47, 127
Turner, D. G., Abdel-Sabour Abdel-Latif, M., & Berdnikov, L. N. 2006, PASP, 118, 410
Turner, D. G., et al. 2008, MNRAS, 388, 444
Wampler, E. J. 1961, ApJ, 134, 861
_________. 1962, ApJ, 136, 100
Wils, P., & Otero, S. A. 2004, Inf. Bull. Variable Stars, 5501, 1

D. G. Turner: Department of Astronomy and Physics, Saint Mary's University, Halifax, Nova Scotia, B3H 3C3, Canada (turner@ap.smu.ca).
R. F. MacLellan, Department of Physics and Engineering Physics, Queen's University, Kingston, ON K7L 3N6 Canada (rmaclellan@bama.ua.edu).
A. A. Henden, American Association of Variable Star Observers, 49 Bay State Road, Cambridge, MA 02138, U.S.A. (arne@aavso.org)
L. N. Berdnikov, Sternberg Astronomical Institute, 13 Universitetskij prosp., Moscow 119992, Russia (leonid.berdnikov@gmail.com).